Cytoskeletal regulation of calcium-permeable cation channels in the human syncytiotrophoblast: role of gelsolin

Nicolás Montalbetti[1], Qiang Li[2], Gustavo A. Timpanaro[1], Silvia González-Perrett[1], Xiao-Qing Dai[2], Xing-Zhen Chen[2] and Horacio F. Cantiello[1,3]

[1] *Laboratorio de Canales Iónicos, Departamento de Fisicoquímica y Química Analítica, Facultad de Farmacia y Bioquímica, Buenos Aires, Argentina*
[2] *Department of Physiology, University of Alberta, Edmonton, Canada*
[3] *Renal Unit, Department of Medicine, Massachusetts General Hospital and, Harvard Medical School, Charlestown, MA 02129, USA*

The human syncytiotrophoblast (hST) is the most apical epithelial barrier that covers the villous tree of the human placenta. An intricate and highly organized network of cytoskeletal structures supports the hST. Recently, polycystin-2 (PC2), a TRP-type nonselective cation channel, was functionally observed in hST, where it may be an important player to Ca^{2+} transport. Little is known, however, about channel regulation in hST. In this report, the regulatory role of actin dynamics on PC2 channels reconstituted from hST apical membranes was explored. Acute addition of cytochalasin D (CD, 5 μg ml^{-1}) to reconstituted hST apical membranes transiently increased K^+-permeable channel activity. The actin-binding proteins α-actinin and gelsolin, as well as PC2, were observed by Western blot and immunofluorescence analyses in hST vesicles. CD treatment of hST vesicles resulted in a re-distribution of actin filaments, in agreement with the effect of CD on K^+ channel activity. In contrast, addition of exogenous monomeric actin, but not prepolymerized actin, induced a rapid inhibition of channel function in hST. This inhibition was obliterated by the presence of CD in the medium. The acute ($<$15 min) CD stimulation of K^+ channel activity was mimicked by addition of the actin-severing protein gelsolin in the presence, but not in the absence, of micromolar Ca^{2+}. Ca^{2+} transport through PC2 triggers a regulatory feedback mechanism, which is based on the severing and re-formation of filamentous actin near the channels. Cytoskeletal structures may thus be relevant to ion transport regulation in the human placenta.

(Resubmitted 21 March 2005; accepted after revision 19 April 2005; first published online 21 April 2005)
Corresponding author H. F. Cantiello: Renal Unit, Massachusetts General Hospital East, Building 149, 13th Street, Charlestown, MA 02129, USA. Email: cantiello@helix.mgh.harvard.edu

The human syncytiotrophoblast (hST) is a differentiated epithelial layer that faces the maternal-facing surface of the human placenta (Enders, 1965; Truman *et al.* 1981; Demir *et al.* 1997). The hST is covered by apical microvilli, which are bathed by the maternal blood. This brush-border epithelial membrane displays a number of transport properties, including the ability to selectively transfer ions (Stulc, 1997). A number of ion channels have been recently identified in hST, and these allow the permeation of cations such as K^+ (Grosman & Reisin, 2000; González-Perrett *et al.* 2001; Llanos *et al.* 2002) and Ca^{2+} (González-Perrett *et al.* 2001), and anions such as Cl^- (Berryman & Bretscher, 2000; Bernucci *et al.* 2003). Little is known, however, about the mechanisms that control and regulate ion channel activity in this syncytial epithelium.

The chorionic villous tree presents an intricate structure, which is continuously growing by branching during gestation (Demir *et al.* 1997). This process requires a dynamic cytoskeleton. The three major cytoskeletal components (Truman & Ford, 1986*a*), microtubules (Smith *et al.* 1977; Douglas & King, 1993), intermediate filaments (Clark & Damjanov, 1985; Hesse *et al.* 2000; de Souza & Katz, 2001), and actin filaments (Beham *et al.* 1988; Parast & Otey, 2000), are present, and may have distinct and interactive roles in the developing placenta. The basal and microvillous plasma membranes of hST exhibit both structural and functional differences. In fact, the apical cytoskeleton encompasses a supermolecular structure, the 'syncytioskeletal layer' of a potentially supporting nature (Ockleford *et al.* 1981). The microvillous actin cytoskeleton may display distinct functional properties, as the apical hST expresses α-actinin (Booth & Vanderpuye, 1983), which is excluded from

N. Montalbetti and Q. Li contributed equally to this work.

DOI: 10.1113/jphysiol.2005.087072

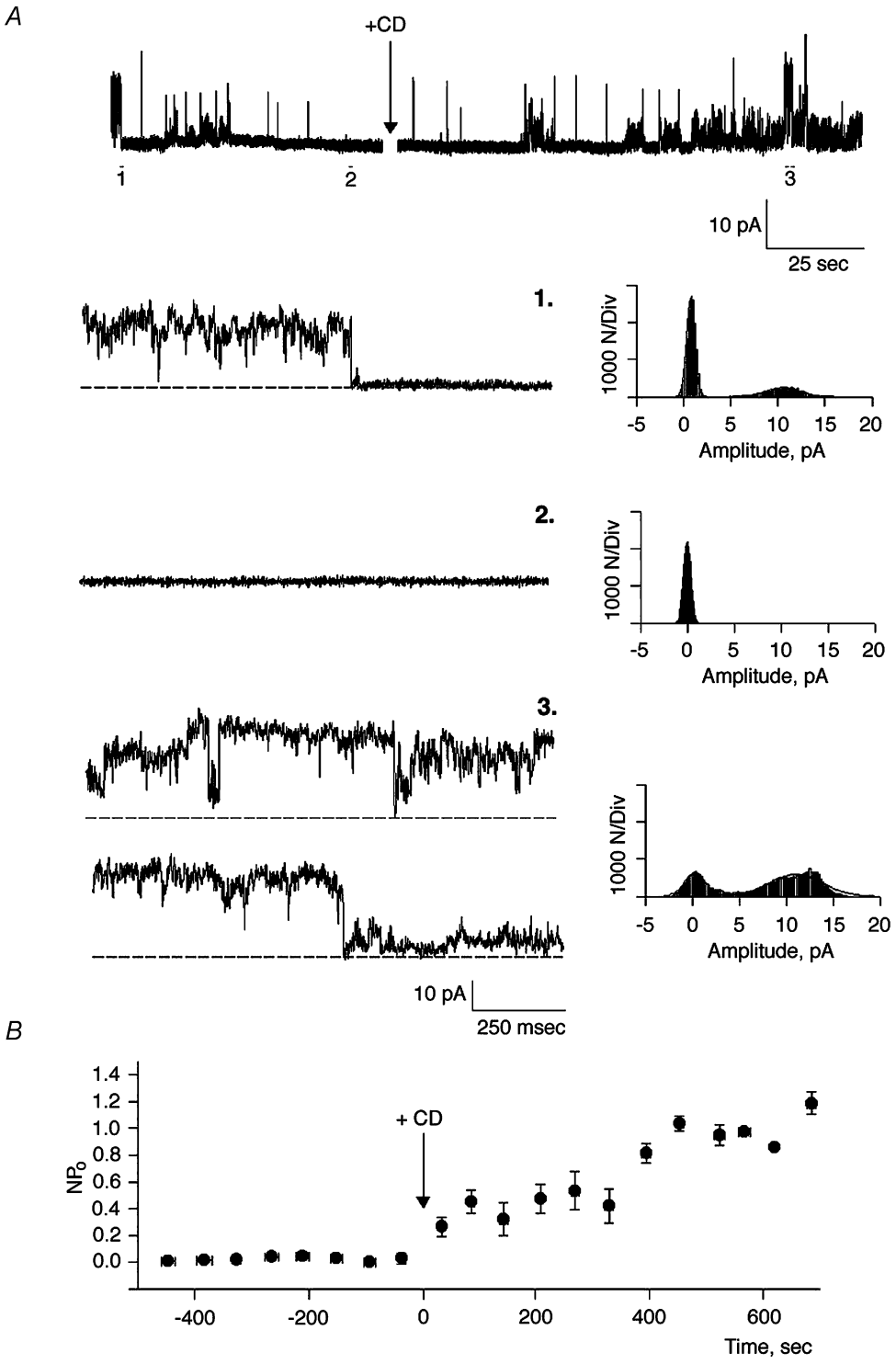

Figure 1. Effect of cytochalasin D on cation channel activity in hST
A, top, representative single-channel tracings of human syncytiotrophoblast (hST) apical membranes. Membranes with spontaneous cation channel activity (1), spontaneously rundown (2), but reactivate after addition of cytochalasin D (CD, 5 μg ml^{-1}) to the *cis* chamber (3). Currents were obtained in the presence of a KCl chemical gradient, with 150 mM KCl in *cis*, and 15 mM *trans*, respectively. Bottom, expanded tracings of single-channel currents (left) for conditions in top tracing. All-point histograms (right) indicate the current amplitude of the CD-activated channels. Channels often showed multiple substates (3, top tracing and histogram). Data are representative of 19 experiments. *B*, average data for mean currents before (negative time), and after addition of CD (arrow). Data are the means ± S.E.M., $n = 5$. Means after addition of CD were statistically different respect to control values ($P < 0.05$).

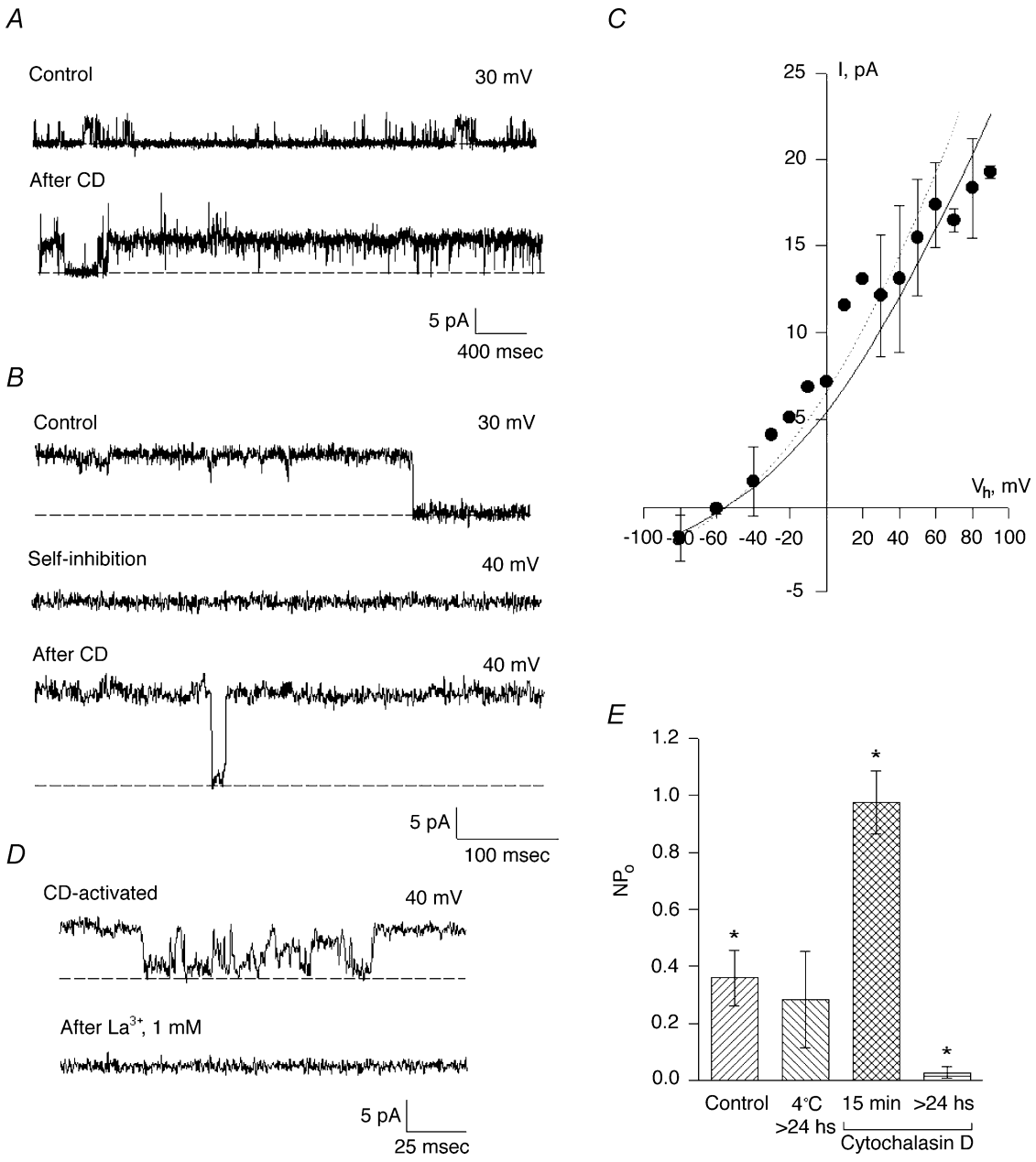

Figure 2. Effect of CD on cation channel activity in hST
A, spontaneous channel activity is increased after addition of CD (5 μg ml^{-1}) to the *cis* chamber (compare top and bottom tracings). The hST apical vesicles were reconstituted in the presence of a KCl chemical gradient, with 150 mM KCl in *cis*, and 15 mM *trans* compartments. Representative tracings show the increase in channel's open probability for the half-conductance substates. Full-size single-channel conductance is observed as spikes in the bottom tracing. Data are representative of seven experiments. *B*, channel activity after spontaneous inhibition also recovered to the maximum conductance state of the channel. *C*, current–voltage relationship for the CD-activated cation-selective channels (observe the reversal potential close to −56 mV, in agreement with E_K, the reversal potential for K^+). The main single-channel conductance was 135 pS. Experimental data (●) are indicated as means ± S.E.M. ($n = 3$). The continuous line is the fitting of data with the Goldman–Hodgkin–Katz (GHK) equation. The dashed line indicates the single-channel conductance of the spontaneously active channel as previously reported (González-Perrett *et al.* 2001). *D*, addition of La^{3+} (1 mM) completely blocked the CD-activated K^+ channel activity in hST. Data are representative of three experiments. *E*, average data for mean currents expressed as $I_m/(V_h - E_k)$ before and after addition of CD. Controls indicate spontaneous activity and the data at 4°C are average data obtained with membranes incubated for more than 24 h at 4°C. Mean currents after addition of CD (15 min) of the drug were statistically different from controls ($P < 0.05$, $n = 8$). However, chronic treatment with CD (>24 h, 4°C) did not maintain an increased activity, consistent with complete disruption of the cytoskeleton. Data are the means ± S.E.M. for eight experiments.

the basal membrane cytoskeleton (Vanderpuye *et al.* 1986). The actin cytoskeleton anchoring protein EBP50 colocalizes with ezrin and actin only in the apical microvilli of the epithelial syncytiotrophoblast (Berryman *et al.* 1995; Reczek *et al.* 1997), and the cytoskeletally related annexins are developmentally expressed in the placenta (Kaczan-Bourgois *et al.* 1996). The differences in membrane-associated cytoskeletal proteins, which correlate with the distinct organizational aspects of actin networks in each membrane domain, may also be a functional effector of ion-channel regulation in the apical aspect of the hST. Apical microvilli have highly organized actin filaments, and are likely to exclude microtubules (Ockleford *et al.* 1981). Further, apical hST membrane preparations present prominent microfilamental structures associated with the presence of structured actin (Smith *et al.* 1977).

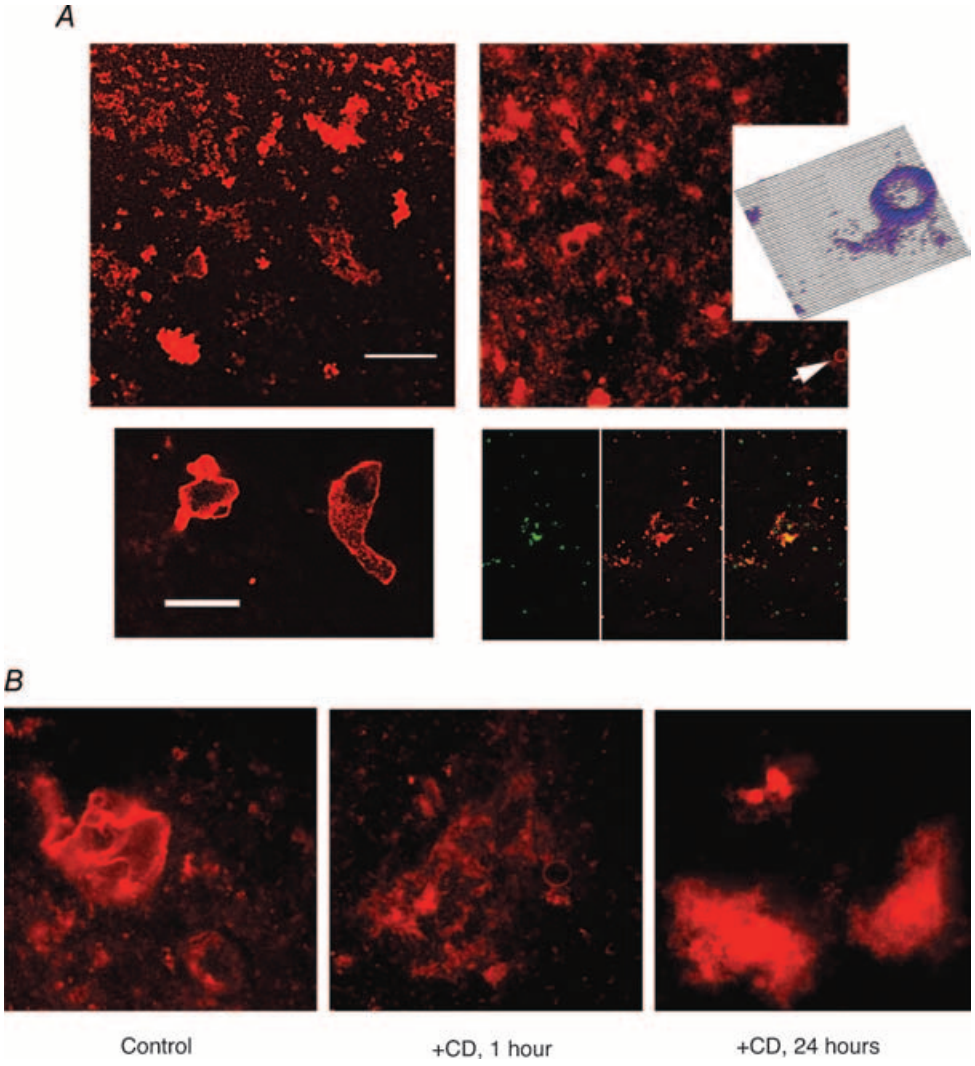

Figure 3. Presence of actin filaments in the hST vesicle preparation
A, the hST apical membrane vesicles were labelled with TRITC-phalloidin (see Methods) to determine the presence of actin filaments in the preparation. Top (left and right), vesicles of various sizes were observed, including large-diameter aggregates (>5 μm diameter, bottom left). The presence of actin filaments was confirmed in all vesicles, with higher concentration of actin filaments in membrane apposition. This is most evident in the inset on top right (arrow and surface plot), and larger vesicles (bottom left). Surface plot was constructed with a subroutine of the public access software Image SXM version 1.62, developed by Steve Barrett (June 1999) of NIH Image. Co-labelling of total actin content (anti-actin antibody, green, left panel) and TRITC-phalloidin (red, middle panel) also indicates concentrated F-actin in the vicinity of the membrane (combined labelling, right panel). Data are representative of duplicate samples from three donor placenta. *B*, effect of CD on hST vesicle actin distribution. Treatment of hST membrane vesicles (left panel) with CD (10 μg ml^{-1}) for either 1 h (middle panel) shows less organized F-actin present. The 24 h treatment (right panel) shows a collapse of the actin cytoskeleton, with almost complete detachment from the membrane.

A body of evidence (reviewed in Cantiello & Prat, 1996; Janmey, 1998) has established a consensus for actin filamental dynamics to play an important role in ion channel regulation in a variety of tissues and cell types. Identifiable ion channels whose function is controlled or regulated by the actin cytoskeleton, include epithelial Na^+ channels (Cantiello *et al.* 1991; Berdiev *et al.* 1996), cystic fibrosis transmembrane conductance regulator (CFTR) (Cantiello, 1996) and other Cl^- channels (Schwiebert *et al.* 1994). Various voltage-gated Na^+ (Undrovinas *et al.* 1996), K^+ (Maguire *et al.* 1998) and voltage-gated Ca^{2+} channels, such as the L-type Ca^{2+} channel of excitable tissues (Johnson & Byerly, 1994; Lader *et al.* 1999), are also subject to regulation by the actin cytoskeleton. This evidence forwards the likely possibility that ion channels are also subject to cytoskeletal regulation in the human placenta. Nonetheless, one of the main problems with this contention is that despite the presence of a variety of ion channels, little is known about the identity of the channel structures underlying channel phenotypes in the syncytiotrophoblast.

In this report, we determined that Ca^{2+}-permeable nonselective cation channels in hST, ascribed to the functional polycystin-2 (PC2), the gene product of *PKD2*, is regulated by changes in the actin cytoskeleton. The presence of actin and the actin-binding proteins, α-actinin and gelsolin, as well as PC2, was confirmed by Western blot and immunofluorescence analyses. Cytochalasin D (CD) treatment modified the organization, but not the total actin content, in the hST vesicle preparation. Addition of actin-filament disrupting agents such as CD, or severing proteins such as gelsolin, activates channel function, which, interestingly was inhibited by addition of monomeric actin. Further, the gelsolin effect was controlled by the channel's ability to transport external Ca^{2+}. Thus, structural changes in cortical actin networks of the apical hST may provide a functional feedback mechanism based on changes in actin filamental dynamics. This function may regulate the hydroelectrolytic homeostasis in the term human placenta.

Methods

Human placenta membrane preparation

Human placenta syncytiotrophoblast apical membrane vesicles were obtained by the method outlined by Booth (Booth *et al.* 1980; Grosman *et al.* 1997), with modifications as recently described (González-Perrett *et al.* 2001). Briefly, term human placentas were obtained under approved institutional guidelines (Maternity Ward and School of Pharmacy and Biochemistry, University of Buenos Aires, Bs. As., Argentina) within 20 min of normal vaginal delivery, and immediately processed. Unless otherwise stated, all steps were carried out at 0°C. Villous tissue samples were fragmented, washed with non-buffered NaCl saline (150 mM), and minced into small pieces. The fragmented tissue was stirred for 1 h in 1.5 vols of a solution containing 10 mM Hepes, adjusted to pH 7.4 with KOH, also containing 0.1 mM EGTA. The solution also contained 0.2 mM phenylmethylsulphonyl fluoride, 1 μg ml^{-1} pepstatin A, 1 μg ml^{-1} aprotinin, 1–5 μg ml^{-1} leupeptin, 1–5 μg ml^{-1} *p*-aminobenzamidine, and 250 mM sucrose. The tissue preparation was filtered through several layers of cheesecloth, and the filtrate was centrifuged for 10 min at 1000 *g*. The supernatant was again centrifuged for 10 min at 14 500 *g*, and for 90 min at 23 400 *g*, in a Sorvall ultracentrifuge with an SS-34 rotor. The final pellet was resuspended in a buffer solution containing 10 mM Hepes-KOH, pH 7.4, 250 mM sucrose, and 20 mM

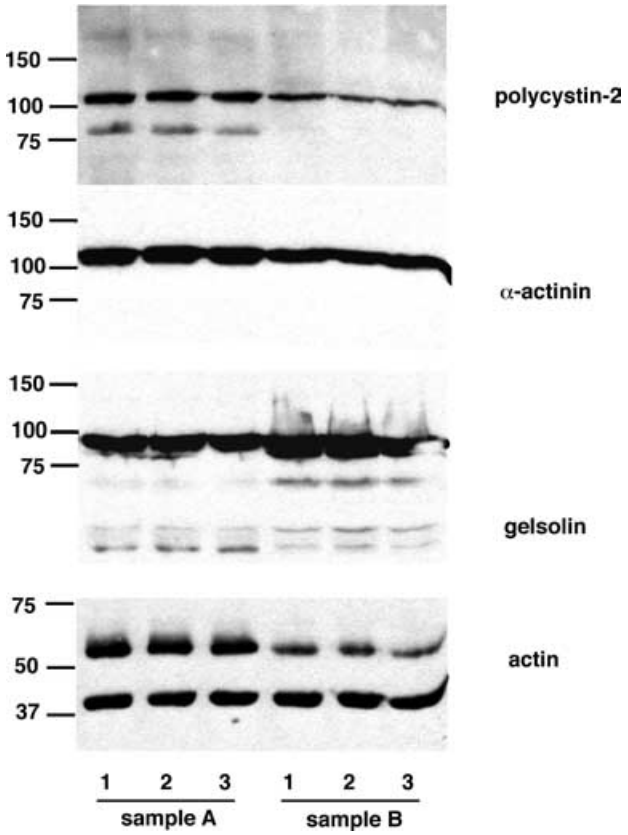

Figure 4. Presence of polycystin-2 (PC2) and actin-binding proteins in hST vesicles
Western blot analysis of hST apical membrane vesicles. The presence of PC2 was confirmed by labelling with an anti-PC2 monoclonal antibody. The vesicles also contained various components of the actin cytoskeleton, including actin, and the actin-associated proteins α-actinin and gelsolin. Data are representative of samples from three donor placenta (two are shown here, *A* and *B*). Treatment of hST membrane vesicles with CD (10 μg ml^{-1}) for either 1 h (labelled '2') or 24 h (labelled '3') had little effect on the total amount of actin and actin-associated proteins present in the vesicle preparation. Control samples are labelled '1'. PC2 channel labelling was also unaffected by CD treatment.

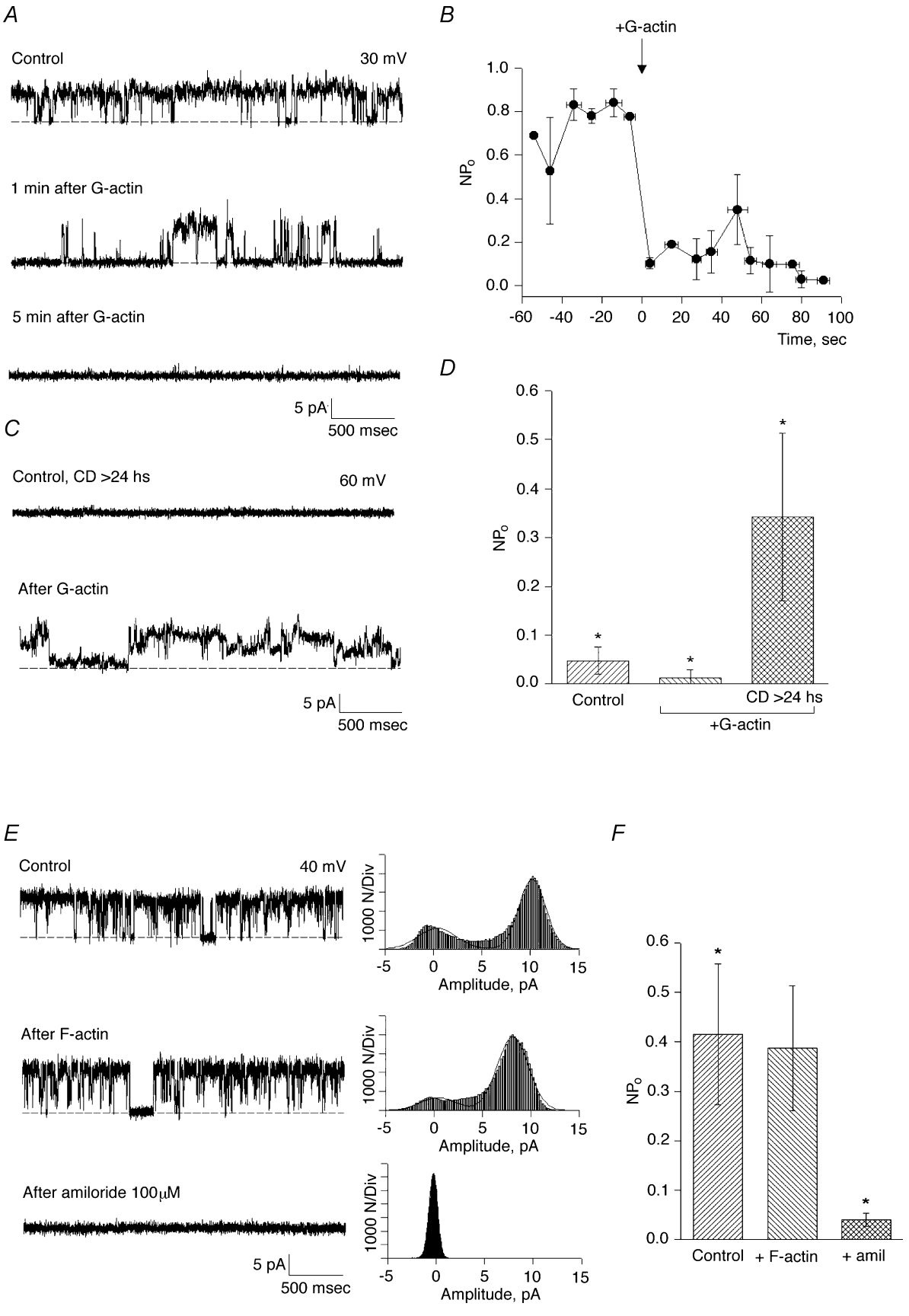

KCl. The membrane suspension was aliquoted and stored at −20°C until the time of the experiment. The apical membrane enrichment (∼26:1 initial homogenate) of the centrifuged fraction was determined by assaying alkaline phosphatase specific activity (Grosman *et al.* 1997). Total protein concentration was determined by the Bradford method (Bradford, 1976). Membrane fractions were reconstituted in a planar lipid bilayer system, as recently described (González-Perrett *et al.* 2001).

Reagents

Specific PC2 labelling in hST apical membranes was conducted with mouse monoclonal anti-PC2 antibody 1A11 originally raised against GST-tagged human PC2 C-terminus (Li *et al.* 2003*a*), and purified for Western blots (WB; 1:1200) and immunofluorescence (IF; 1:30). Functional studies with anti-PC2 antibody were conducted with a polyclonal antibody raised against a bacterial fusion protein containing the C-terminal 258 aa of human PC2 (1:10 dilution) a kind gift of Dr Peter Harris, Mayo Clinic, Minneapolis, MN, USA, as originally reported (Ong *et al.* 1999). This antibody inhibits human PC2 as reported (González-Perrett *et al.* 2001). Mouse monoclonal anti-α-actinin BM75.2 and anti-gelsolin antibodies, and rabbit polyclonal anti-actin antibody (Sigma-Aldrich, Canada) were used for WB. Rabbit anti-α-actinin serum (Sigma-Aldrich) and anti-actin antibody were used for IF. Secondary antibodies were used as follows: goat anti-mouse IgG fluorescein isothiocyanate and goat anti-rabbit IgG-rhodamine (Chemicon International, Temecula, CA, USA) were used for IF; goat anti-mouse and rabbit IgG-horseradish peroxidase (HRP; Chemicon International), were used for WB. Phalloidin-tetramethyl-rhodamine B isothiocyanate (TRITC; Sigma-Aldrich) was used to stain filamentous actin. Actin was obtained from original vendors (Sigma; Cytoskeleton, Boulder, CO, USA) without further purification. G-actin (monomeric, 5–10 mg ml^{-1}) was stored at −80°C in a depolymerizing buffer containing (mM): 2.0 Tris-HCl, 0.5 ATP, 0.2 $CaCl_2$, and 0.5 β-mercaptoethanol, pH 8.0. CD (Sigma) was dissolved in DMSO and used at concentrations ranging from 1 to 50 μM. Gelsolin (1 mg ml^{-1} in PBS) was obtained from Cytoskeleton. Gelsolin was further dissolved in '*trans*' saline and used at final concentrations ranging from 40 to 600 nM.

Protein immunoblotting

hST apical membrane vesicles were treated with 10 μg ml^{-1} CD (Sigma-Aldrich) at 4°C for 1 and 24 h. Control and CD-treated vesicles were subjected to 8% SDS-PAGE electrophoresis and transferred to nitrocellulose membranes (Amersham, Baie d'Urfe, Canada). The membranes were then blocked with 3% skim-milk powder in phosphate-buffered solution (PBS) supplemented with 0.1% Tween-20, incubated with a primary antibody and an HRP-coupled secondary antibody, and visualized with enhanced chemiluminescence (Amersham).

Immunofluorescent staining

All steps were conducted at room temperature. hST vesicles were placed in Eppendorf tubes (1.5 ml total volume), diluted in 10% mouse and/or rabbit sera in PBS, and incubated for 30 min to prevent nonspecific binding of

Figure 5. Effect of actin on cation channel activity in hST
A, representative single-channel tracings of hST apical membranes in asymmetrical KCl. The hST apical vesicles were reconstituted in the presence of a KCl chemical gradient, with 150 mM KCl in *cis*, and 15 mM *trans* compartments. Membranes with spontaneous ion channel activity were first obtained (top tracing). Addition of actin (1 mg ml^{-1}) to the *cis* chamber inhibited cation-selective ion channel activity (the bottom two tracings). Data are representative of 17 experiments. *B*, effect of G actin on average channel activity (expressed as NP_o, where N is the total number of active channels, and P_o is the open probability of the open channel). Actin inhibited channel activity within 1 min of addition (arrow). Data are the means ± S.E.M. ($n = 5$). All values after actin addition are statistically different from controls (indicated as negative time). *C*, addition of actin to CD-treated membranes (>24 h), in contrast, stimulated otherwise quiescent apical membranes. Channel activity in the reconstituted membrane was first determined by sporadic flickering prior to actin addition (data not shown). *D*, summarized data are indicated as means ± S.E.M. for control conditions ($n = 7$), and after addition of actin to acutely (<15 min, centre, $n = 7$) and chronically (>24 h, right, $n = 3$) CD-treated membranes. While actin addition was inhibitory to control membranes, the same actin concentration was stimulatory in chronically CD-treated membranes ($P < 0.05$ in both cases). *E*, representative single-channel tracings of hST apical membranes in asymmetrical KCl. The hST apical vesicles were reconstituted in the presence of a KCl chemical gradient, with 150 mM KCl in *cis*, and 15 mM *trans* compartments. Membranes with spontaneous ion channel activity were first obtained (top tracing). Addition of prepolymerized actin (2 h in 150 KCl plus 1 mM $MgCl_2$) to the *cis* chamber was without effect on cation-selective ion channel activity (middle tracing). Channel activity was readily inhibited by amiloride (100 μM, bottom tracing). Data are representative of 5 experiments. All-point histograms to the right of each tracing indicate current amplitude. *F*, average data for membrane currents expressed as the means ± S.E.M. of NP_o ($n = 5$).

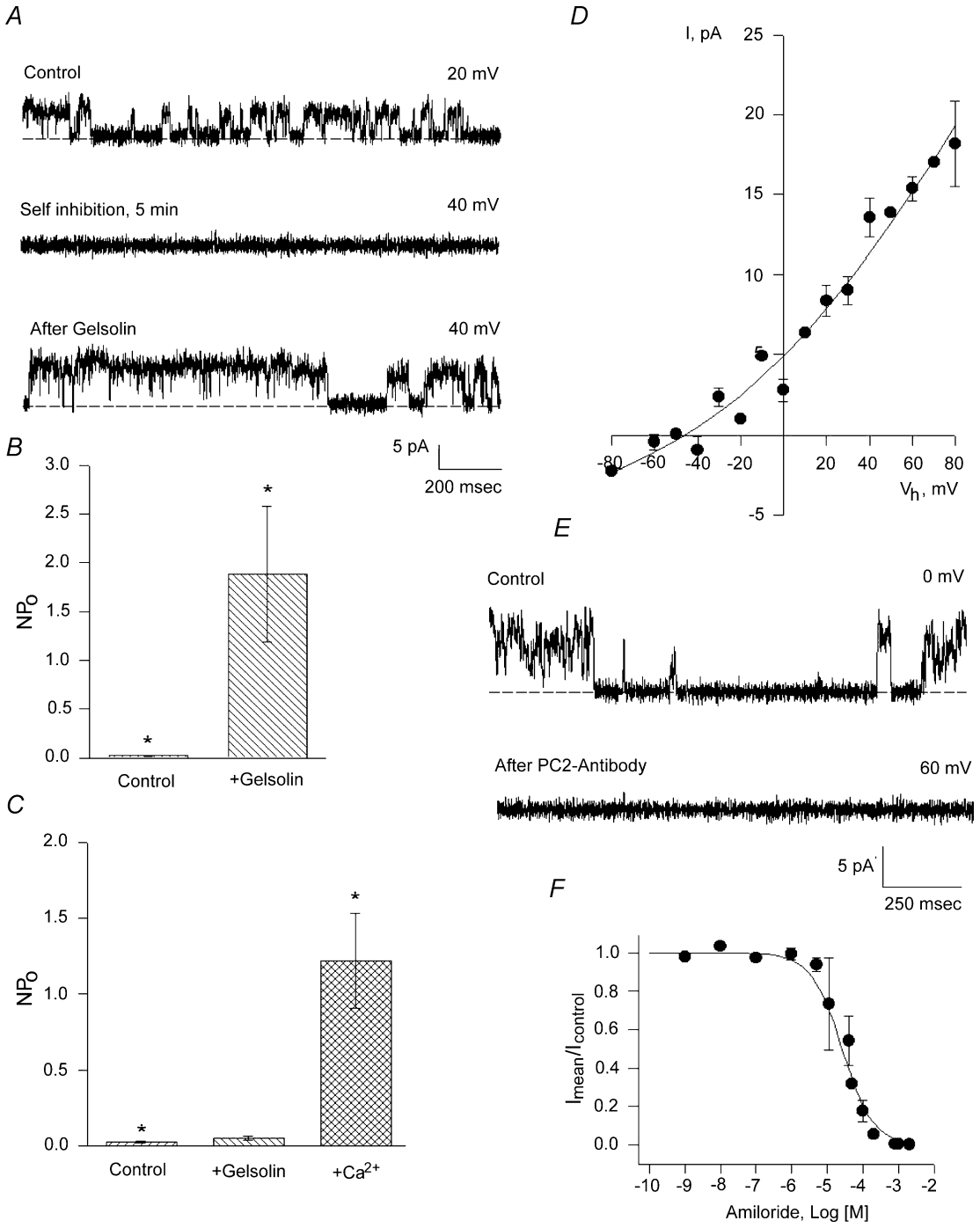

Figure 6. Effect of gelsolin on cation channel activity in hST

A, the Ca^{2+}- and pH-dependent actin-severing protein gelsolin re-activated previously rundown K^+-permeable channels in hST membranes. This effect was observed under control conditions in the presence of 10 μM Ca^{2+}. Data are representative of 7 experiments. *B*, average data indicating the increase in cation-selective channel activity after addition of gelsolin. The data indicate that in the presence of Ca^{2+}, activated gelsolin acts in a CD-like fashion. Data are the means ± S.E.M. of 13 and 6 experiments, for control and gelsolin-treated membranes, respectively. *C*, in a Ca^{2+}-free solution (control), however, gelsolin addition (+gelsolin) was unable to induce channel activation. Further addition of Ca^{2+} to the *cis* chamber (Ca^{2+}) restored the stimulatory effect of gelsolin. Data are representative of 5 experiments. *D*, single-channel conductance of gelsolin-activated K^+-permeable channels. Experimental data (●) are the means ± S.E.M. of 5 experiments. Data were obtained in a K^+ gradient as in Figs 1 and 2, and fitted with the GHK equation (continuous line). *E*, gelsolin-activated channels were inhibited within seconds by addition of anti-PC2 antibody (1:10 dilution, $n = 3$). *F*, dose–response for inhibitory effect of various concentrations of amiloride. Experimental data (●) are the means ± S.E.M. of 5 experiments. Data were fitted with an equation of binding with a single inhibitory site, which rendered a $K_i = 24$ μM.

antibodies. PBS containing 2% BSA was used for antibody dilution and washing. Vesicles were treated with primary antibodies for 1 h, rinsed three times by centrifugation and supernatant removal, and incubated with secondary antibodies for 45 min. This procedure was followed by another washing (×3) with PBS. Pelleted vesicles were transferred to glass slides, mounted with Vectashield mounting medium (Vector Laboratories, Burlingame, CA, USA), and sealed with clear nail varnish. Immunofluorescence was visualized with a Zeiss 510 confocal laser scanning microscopy with argon 488 nm and helium–neon 543 nm lasers (Zeiss, Weesp, The Netherlands). TRITC-phalloidin staining was visualized with a helium–neon 543 nm laser. Surface plots of stained vesicles were constructed by first obtaining a grey-scale profile of the picture. The surface plot of the grey-scale image was then obtained by smooth filtering, followed by application of the surface plot subroutine of the

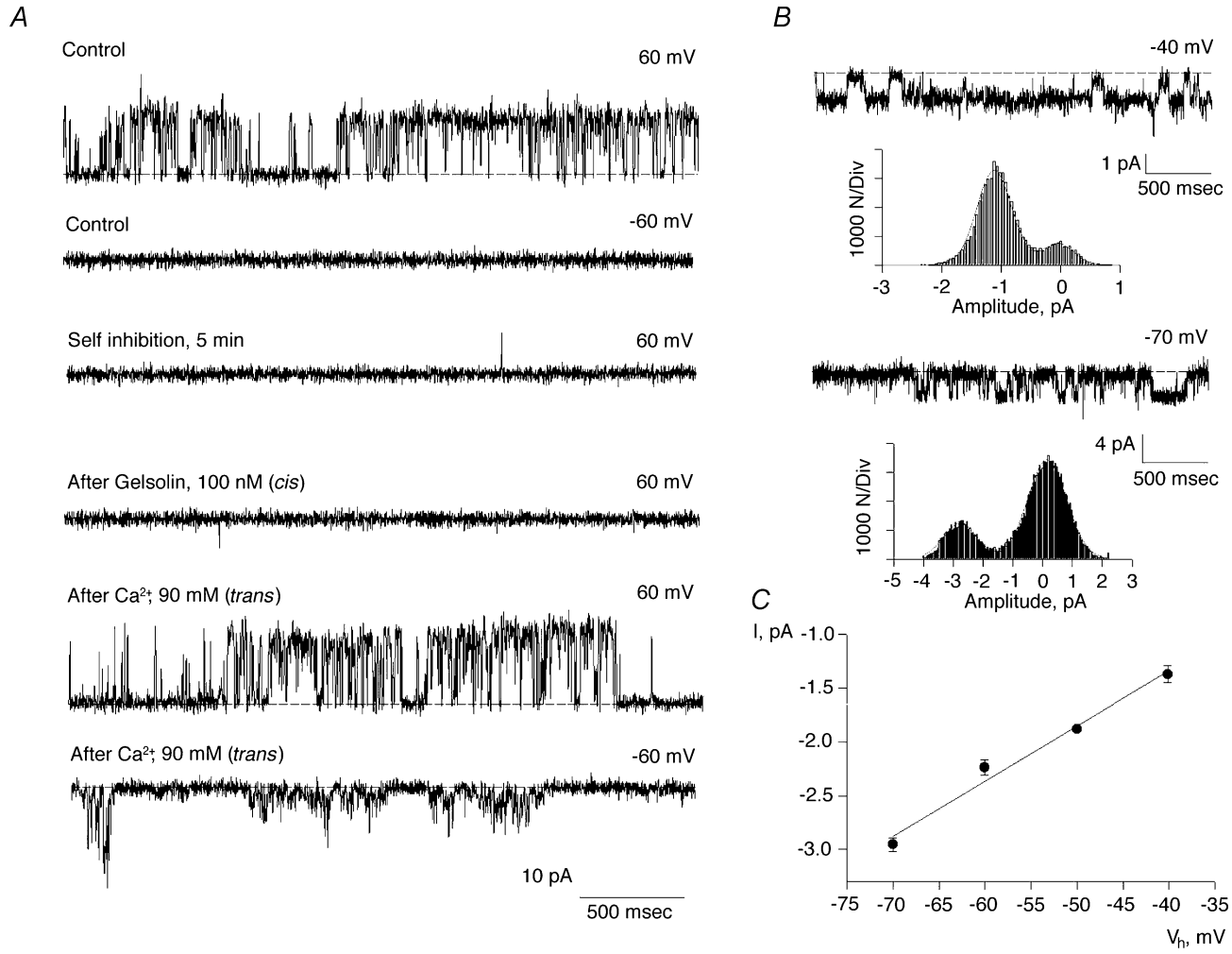

Figure 7. Effect of Ca^{2+} transport on the gelsolin regulation of hST cation channels
A, representative single-channel tracings of hST apical membranes in asymmetrical KCl. The hST apical vesicles were reconstituted in the presence of a KCl chemical gradient, with 150 mM KCl in *cis*, and 15 mM *trans* compartments in the absence of Ca^{2+}. Membranes with spontaneous ion channel activity were first obtained. See the top two tracings for +60 and −60 mV. Cation channel activity was not observed at negative potentials as the holding potential is close to the E_K (control, second tracing). Upon return to positive potentials (+ 60 mV), channels do not re-activate as previously reported (Xu *et al.* 2003). Further addition of gelsolin under these conditions did not re-activate channel function (fourth tracing). However, addition of Ca^{2+} (90 mM) to the *trans* chamber, re-activated channel activity in the presence, but not the absence of *cis* gelsolin. The data indicate that Ca^{2+} transport feeds back into gelsolin activation, and thus re-initiation of hST cation channel activity. Data are representative of 5 experiments. *B*, single-channel currents immediately after addition of Ca^{2+} (90 mM) to the *trans* compartment. *C*, Ca^{2+} currents initially had a 51 pS single-channel conductance, which further decreased in the presence of 90 mM Ca^{2+} in the *trans* compartment (see Fig. 8). Please note the *trans* compartment also contained 15 mM KCl. Experimental data (●) are the means ± S.E.M. ($n = 3$), and they were fitted to a straight line (continuous line).

public access software Image SXM version 1.62, developed by Steve Barrett (June 1999) from NIH Image. Final composite images were created using Adobe Photoshop 5.5.

Ion-channel reconstitution

Lipid bilayers were formed with a mixture of synthetic phospholipids (Avanti Polar Lipids, Birmingham, AL, USA) in *n*-decane as reported (González-Perrett *et al.*

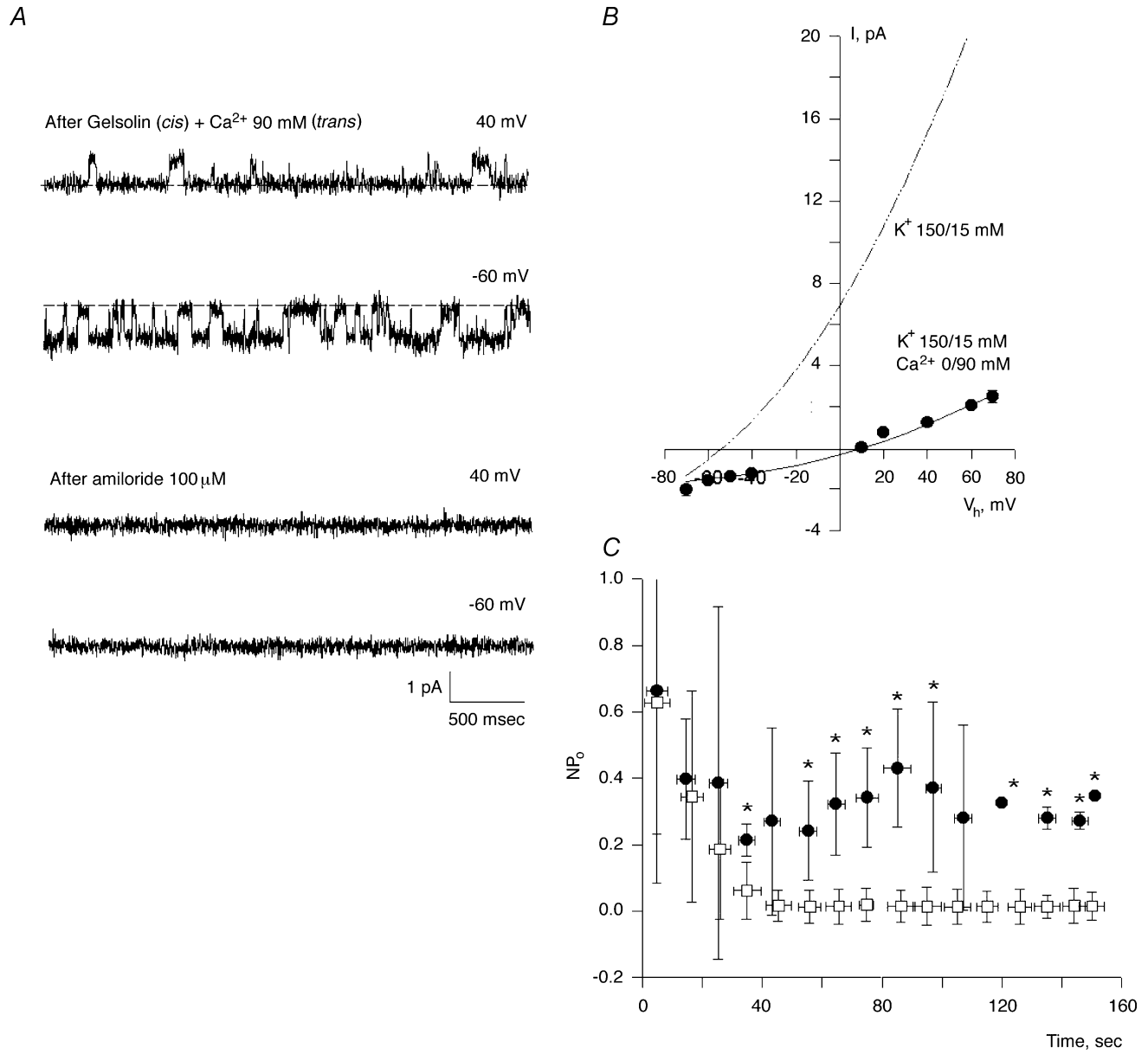

Figure 8. Effect of Ca^{2+} transport on gelsolin-activated hST cation channel activity
A, representative single-channel tracings of hST apical membranes in asymmetrical KCl (150 mM KCl) in *cis*, and 15 mM KCl and 90 mM $CaCl_2$ in *trans* compartments. Data are representative of 9 experiments. Channel activity was observed in the presence of gelsolin (*cis*, 100 nM) after addition of Ca^{2+} to the *trans* compartment. Addition of amiloride (100 μM) to the *trans* compartment induced a simultaneous inhibition of both K^+ and Ca^{2+} currents (bottom tracings). Data are representative of 3 experiments. *B*, Ca^{2+} transport through the channel further reduces the single-channel conductance to 21 pS (see Fig. 7 for comparison), and induces a shift of approximately 60 mV in the reversal potential (−54 to >+10 mV). *C*, the presence of gelsolin (100 nM, ●) in the *cis* compartment decreases the inhibitory effect of K^+ transport (□) through cation-permeable channels in hST. Data are the means ± S.E.M. ($n = 5$), and they were obtained as NP_o of current activity at positive potentials. Asterisks indicate statistical difference at least $P < 0.05$.

2001). The lipid mixture was made of 1-palmitoyl-2-oleoyl phosphatidylcholine and phosphatidylethanolamine in a 7:3 ratio. The lipid solution (∼20–25 mg ml^{-1}) in *n*-decane was spread in the aperture of a polystyrene cuvette (CP13-150) of a bilayer chamber (model BCH-13; Warner Instruments, Hamden, CT, USA). Both sides of the lipid bilayer were bathed with a solution containing 10 mM MOPS-KOH and 10 mM MES-KOH, pH 7.40, and 10–15 μM Ca^{2+}. The final K^+ concentration in the solution was approximately 15 mM. KCl was further added to the *cis* compartment where membrane vesicles were fused, such that final concentrations of 150 K^+, and 135 Cl^- were achieved in this side of the chamber.

Changes in Ca^{2+} concentrations

Most experiments, including those under control conditions, were conducted in the presence of symmetrical Ca^{2+} (10 μM), namely on both the *cis* and *trans* chambers. Whenever indicated, a Ca^{2+}-free solution in which Ca^{2+} was eliminated by adding EDTA (10 mM) to the *cis* (intracellular) compartment was used. This was done with or without 10 μM Ca^{2+}. To assess the effect of *trans* ('extracellular') Ca^{2+} under the *cis* Ca^{2+}-free conditions (see above) through the hST cation channels, an aliquot of concentrated $CaCl_2$ was added to the *trans* chamber to reach a final concentration of 90 mM, as originally reported (González-Perrett *et al.* 2001). This was done with the expectation that Ca^{2+} transport through the hST cation channels would activate the gelsolin placed in the *cis* compartment (see Results).

Data acquisition and analysis

All the experiments were performed at room temperature (20–25°C). Electrical signals were obtained with a PC501A patch-clamp amplifier (Warner Instruments) with a 10 GΩ feedback resistor. Output (current and voltage) signals were low-pass filtered at 700 Hz (−3 dB) with an eight-pole Bessel-type filter (Frequency Devices, Haverhill, MA, USA). Signals were displayed on an oscilloscope. Single-channel current tracings were further filtered for display purposes only. Unless otherwise stated, pCLAMP version 5.5.1 (Axon Instruments, Union City, CA, USA) was used for data analysis, and Sigmaplot Version 2.0 (Jandel Scientific, Corte Madera, CA, USA) for statistical analysis and graphics. Single-channel conductances under asymmetrical conditions were calculated by the best fitting of current-to-voltage experimental data to the Goldman–Hodgkin–Katz (GHK) equation, as recently reported (González-Perrett *et al.* 2001). Each reconstituted

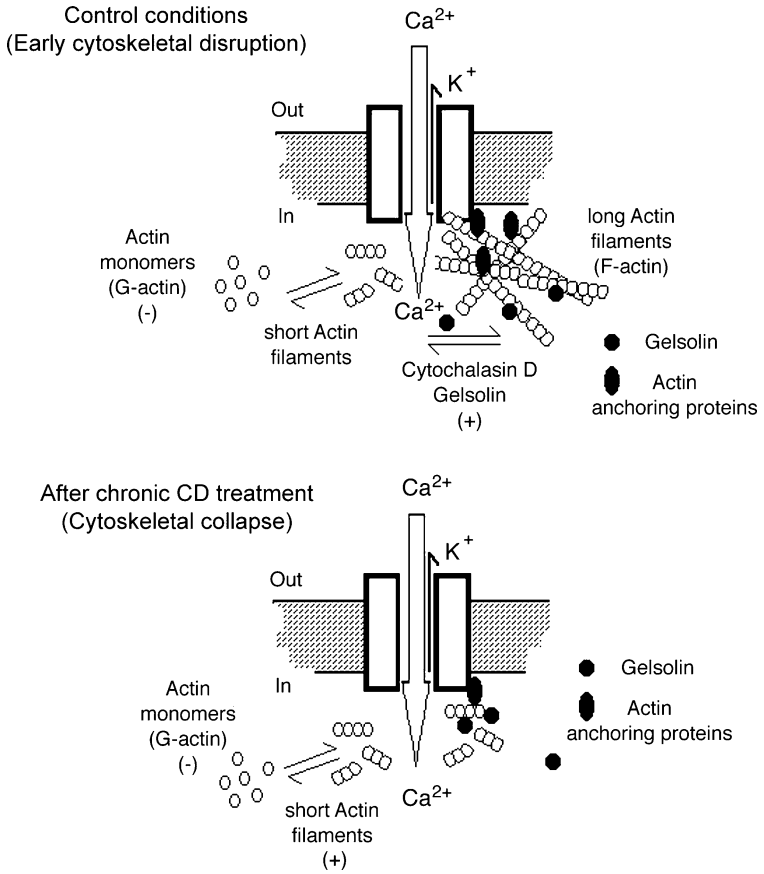

Figure 9. Schematic model of regulation by the actin cytoskeleton of cation channels in hST
Top, in the hST of term placenta, the actin cytoskeleton comprises an intracellular superstructure composed of actin and actin-binding proteins. Actin is found as long filaments (F-actin) associated to the membrane-embedded channels, which are tonically silent as a result of this actin conformation. F-actin disorganization by toxins, such as CD, and actin-severing proteins, such as gelsolin, plus Ca^{2+} initiates channel activity, which in turn is modulated by Ca^{2+} transport through these nonselective cation channels. Monomeric (G) actin has an inhibitory effect under control conditions, which is likely to be by competition with previously resident, prepolymerized actin. Bottom, addition of G-actin after chronic CD treatment, which renders a collapsed cytoskeleton and low channel activity is, in contrast, able to re-activate channel function. This is likely to be accounted for by a replenishing of F-actin in the vicinity of the channels. The encompassed data indicate that Ca^{2+} transport through the channels elicits a feedback mechanism that is mediated by the Ca^{2+}-induced activation of proteins such as gelsolin, which in turn modulate hST cation channel activity through the cytoskeleton.

lipid–protein membrane preparation contained at least three variables: the number of active ion channels, different single-channel currents due to multiple substates (González-Perrett *et al.* 2002) and distinct open probabilities under each condition. Thus, the data were analysed as recently described (Xu *et al.* 2003). Briefly, the mean membrane current was obtained for each reconstituted membrane (12.5 s), prior to averaging data for each condition. Thus, the data, although indicated as currents (picoamps) represents either the current density (12.5 s per membrane), or average conductance by dividing this value by the holding potential $V_h - E_k$ (the reversal potential for K^+). The mean data under each condition are thus represented by $I = NiP_o$. Where N is the total number of active channels, i is the average single-channel current for the channel species, and P_o is the open probability of the open channel, at a given holding potential (as indicated above). NiP_o values were often calculated from shorter tracings than those used for mean currents, in particular those in which single-channel levels could be defined (small N), and the P_o could be directly assessed from the tracing. This was particularly useful in conditions under which the channel showed more than one subconductance state, where each level was considered independently. Whenever indicated, statistical significance was obtained by unpaired Student's test comparison of sample groups of similar size. Average data values were expressed as the mean ± S.E.M. (n) under each condition, where n represents the total number of experiments analysed. Statistical significance was accepted at $P < 0.05$ as calculated by paired Student's test (Snedecor & Cochran, 1973).

Calculation of cationic perm-selectivity ratios

The single-channel conductance was calculated as previously reported (González-Perrett *et al.* 2001) by fitting experimental data to either a straight line (symmetrical cations) or the GHK equation (asymmetrical cation concentrations). Ionic perm-selectivity ratios were calculated with a modified version of the GHK (Hille, 1992), where the P_{Ca}/P_K ratio was fitted to the experimental data in the presence of K^+ and Ca^{2+}, with:

$$\{1 + \exp(-FV/RT)(K_c - K_t[\exp(-FV/RT)])\}/$$
$$\{4([Ca_t \exp(-2FV/RT)] - Ca_c)\}$$

where c is *cis* chamber, t is *trans* chamber, V is reversal potential, F is Faraday's constant, R is the gas constant, T is absolute temperature, and K and Ca are the mean activities for the K^+ and Ca^{2+} ions, respectively. A similar approach was conducted for other mono–divalent cation interactions. Data are expressed as the means ± S.E.M.

Results

Effect of CD on channel activity in hST

To assess a regulatory role of the actin cytoskeleton on channel function in hST, apical vesicles were reconstituted in a lipid-bilayer system. Experiments were conducted in the presence of a K^+ chemical gradient, with 150 mM KCl in the *cis* compartment, and 15 mM KCl in the *trans* compartment (Fig. 1). Reconstituted membranes were chosen if they displayed spontaneous cation-selective ion channel activity at the beginning of the experiment (Fig. 1*A*). Often, spontaneous channel activity decreased (rundown) during the course of the experiment. In 17 out of 19 experiments, addition of CD (5 μg ml^{-1}) to the *cis* compartment re-initiated K^+-permeable ion currents (Fig. 1*A*). CD-activated membrane currents increased eightfold from 0.023 ± 0.019 to 0.217 ± 0.154 pA ($n = 8$, $P < 0.01$) at 7.42 ± 0.28 min ($n = 5$) after exposure to the drug (Fig. 1*B*). The CD effect was also manifested by an increased P_o of open substates (Fig. 2*A*). Moreover, CD addition even caused rundown channels to re-open to their maximal single-channel conductance (Fig. 2*B*). Currents were cation selective, with a high K^+/Cl^- perm-selectivity ratio (see reversal potential, Fig. 2*B*), and a maximal single-channel conductance of 135 ± 7 pS ($n = 3$, Fig. 2*C*). Channels were inhibited by La^{3+} (500 μM, Fig. 2*D*) and amiloride (50 μM, data not shown). These currents thus displayed the main characteristics of those previously reported for PC2 in hST (González-Perret *et al.* 2001). To further test the role of endogenous actin filaments on cation channel activity, hST apical membranes were incubated for 1–3 days at 4°C in the presence of CD (5 μg ml^{-1}) to completely collapse the actin networks. Channel activity was largely abolished in the chronically CD-treated membranes (Fig. 2*E*), which only displayed flickery and sporadic channel openings (data not shown).

Presence of actin and actin-binding proteins in hST membrane vesicles

To assess the presence of cytoskeletal proteins in the enriched hST vesicle preparations used for the functional studies, we conducted immunofluorescence and Western blot analyses (Figs 3 and 4). The hST vesicles from three independent donors were used for these studies, with largely similar findings in all preparations. All vesicles (of different sizes) showed strong TRITC-phalloidin labelling (Fig. 3, top), supporting the presence of filamentous (F) actin in the preparation. This was confirmed by colabelling of TRITC-phalloidin and anti-actin antibodies to label F-actin, and the entire actin pool, respectively. F-actin labelling was strongest in proximity to the membrane (Fig. 3, top, inset). This is in agreement with previous

findings showing an organized actin cytoskeleton in apposition to the plasma membrane in hST apical vesicles (Booth *et al.* 1980; Bloxam *et al.* 1997*a*,*b*; Grosman *et al.* 1997; Smith *et al.* 1977). A 1 h incubation of hST apical membranes with CD (10 μg ml^{-1}, Fig. 3, bottom) affected the presence of F-actin in the vicinity of the membrane. This could only be observed in the larger vesicles. An extended incubation with CD (10 μg ml^{-1} for 24 h), further collapsed the cytoskeleton where most actin was 'detached' from the plasma membrane. Western blot analysis (Fig. 4) identified the presence of actin and the actin-binding proteins α-actinin and gelsolin, as well as the channel PC2, suggesting a functional interface between the PC2 channel and the actin cytoskeleton. A comparison between control and CD-treated samples indicated that the total amount of protein remained largely the same in all three preparations. These data are in agreement with previous evidence indicating the presence of organized actin filaments in hST (Smith *et al.* 1977; Truman *et al.* 1981; Booth & Vanderpuye, 1983; Truman & Ford, 1984, 1986*a*,*b*; Demir *et al.* 1997; Grosman *et al.* 1997; Kingdom *et al.* 2000).

Actin regulation of cation channels in hST

To assess whether the stimulatory effect of CD on K^+ channel activity in hST was induced by short actin filaments produced by the drug, or released monomers, the effect of nonpolymerized actin on channel function was determined. Addition of a polymerizable concentration of exogenous (G) actin (1 mg ml^{-1}) to spontaneously active control hST apical membranes, inhibited K^+ channel activity in 15 out of 17 experiments (Fig. 5*A*). The mean membrane current decreased by 74.2%, from 0.048 ± 0.011 pA, $n = 5$, to 0.012 ± 0.007 pA, $n = 5$ ($P < 0.03$). This inhibitory effect was observed within 20 s after the addition of actin (Fig. 5*B*). Addition of prepolymerized (F) actin, however, had no effect (Fig. 5*E*–*F*). The inhibitory effect of G-actin was not observed in the presence of CD (<15 min), in which channel activity remained high (data not shown). This is interesting, since CD helps nucleate and polymerize (although not elongate) actin (Goddette & Frieden, 1986). In chronically CD-treated membranes (>24 h), however, channel activity was re-activated by addition of a similar concentration of G-actin (1 mg ml^{-1}, Fig. 5*C*). This is consistent with the polymerization of actin in the vicinity of the channels, which are now devoid of endogenous F-actin. In three out of three experiments, membrane currents increased from 0.005 ± 0.001 to 0.26 ± 0.014 pA, $n = 3$, $P < 0.05$ (Fig. 5*D*) after addition of actin. These data suggest competition of exogenous (monomeric) actin with the endogenous pool of actin filaments and likely channel-associated proteins.

Effect of gelsolin on the cytoskeletal regulation of K^+-permeable channels in hST

The above data indicate the presence and regulatory effect of a pool of endogenous actin and associated proteins in the cation channel activity of hST membranes, where the presence of PC2 channels was also determined. The data support the fact that changes in actin cytoskeletal dynamics plays a functional role in K^+ channel regulation in hST apical membranes. To further test whether severing endogenous actin filaments mediates this regulation in hST, we also assessed the effect of the Ca^{2+}-dependent actin-severing protein, gelsolin (Yin *et al.* 1981; Kwiatkowski & Yin, 1987). Gelsolin labelling was confirmed for the first time in the hST apical membrane preparation (Fig. 3). Addition of gelsolin (40 nM) to control membranes, in which the Ca^{2+} concentration in the *cis* compartment was kept at 10 μM, increased K^+ channel activity in 15 out of 16 experiments (Fig. 6*A*). This Ca^{2+} concentration was similar to that used for assessing hST spontaneous K^+ channel activity (González-Perrett *et al.* 2001). Membrane currents increased 87-fold, from 0.049 ± 0.025 to 4.30 ± 2.40 pA, $n = 10$, for control *versus* gelsolin-treated membranes, respectively ($P < 0.05$, Fig. 6*B*). Addition of gelsolin, in the absence of Ca^{2+} (via chelation with EDTA 10 mM), however, was without effect on channel activity (0.031 ± 0.039 pA, $n = 10$, *versus* 0.032 ± 0.026 pA, $n = 8$, $P < 0.2$, Fig. 6*C*), consistent with the gelsolin's known Ca^{2+} dependence. This effect was reversed by addition of Ca^{2+} to the *cis* compartment (3.507 ± 1.47 pA, $n = 7$, $P < 0.001$, Fig. 6*C*). The gelsolin-activated cation channels had a single-channel conductance of 135 pS (Fig. 6*D*), and were inhibited by anti-PC2 antibodies (Fig. 6*E*). Addition of the antibody to the *cis* compartment blocked channel activity within seconds, thus following a time response entirely different from that observed with rundown kinetics. Addition of unrelated anti-flag antibody was without effect, indicating that the effect was specific for PC2 (data not shown). Amiloride, added from the *trans* compartment, also blocked cation channel activity (Fig. 6*F*). The inhibitory constant for amiloride calculated from a dose–response was 24 μM, in close agreement with that reported for spontaneous cation channel activity in hST (González-Perrett *et al.* 2001). Interestingly, the lack of gelsolin effect in the absence of *cis* Ca^{2+} (Fig. 7*A*) reversed (in 7 out of 9 experiments) after further addition of Ca^{2+} (90 mM) to the *trans* chamber, presumably because of Ca^{2+} transport from *trans* to *cis* compartments through the channels. This was confirmed by the observation of Ca^{2+}-permeating currents (negative potentials), which increased to 1.22 ± 0.69 pA, $n = 5$ ($P < 0.01$) immediately after addition of *trans* Ca^{2+} (Fig. 7*B*). The single-channel conductance of the Ca^{2+} currents was 51 pS (Fig. 7*C*). Ca^{2+} transport was mediated

through the K^+-permeable channels (Fig. 8*A*). This was confirmed by the observation of single-channel currents in opposite directions for positive and negative potentials, and the simultaneous inhibition of both inwardly (Ca^{2+}-carrying) and outwardly directed (K^+-carrying) currents in the presence of external (*trans*) amiloride (100 μM, Fig. 8*A*). In the presence of high external Ca^{2+} (90 mM), the single-channel conductance further decreased to 21 pS, with a strong shift in reversal potential (Fig. 8*B*), consistent with direct competition between the two charge carriers, as originally reported for the spontaneous cation channel activity (González-Perrett *et al.* 2001). Interestingly, channel activity, as assessed by the NP_o of the K^+-carrying currents of reconstituted membranes in the presence of external high Ca^{2+} (90 mM), was much higher in the presence of exogenous cytoplasmic gelsolin (40 nM). The data are most consistent with a feedback mechanism, where the transported Ca^2 through the K^+-permeable channels is regulated by remodelling of the actin cytoskeleton via activation of 'cytoplasmic' gelsolin. This regulation counters the inhibitory effect of Ca^{2+}on the channel (Ca^{2+}-induced Ca^{2+} inhibition).

Discussion

In the present study, we demonstrate that dynamic changes in the endogenous actin cytoskeleton regulate K^+- and Ca^{2+}-permeable cation channels in the human syncytiotrophoblast. The actin-severing protein gelsolin in the presence, but not absence of Ca^{2+}, endogenously mediates this effect. Thus, the activation of these cation channels by the Ca^{2+}–gelsolin complex, but not gelsolin alone, indicates that the cleavage of endogenous actin filaments by Ca^{2+}-activated gelsolin is a triggering mechanism, in agreement with the acute effect of CD. Thus, the expected activation of gelsolin by the transported Ca^{2+} through the channels further supports a feedback mechanism. This feedback mechanism involves channel-associated proteins (Fig. 9), whose role accounts for the reversal of the inhibitory effect elicited by Ca^{2+} on the channels themselves (Ca^{2+}-induced Ca^{2+} inhibition). Interestingly, addition of monomeric actin had a largely inhibitory effect under control conditions, in contrast to the stimulatory effect observed after complete collapse of the endogenous cytoskeleton induced by a chronic CD incubation period (>24 h). This seemingly contradictory phenomenon may be explained by competition of G-actin with the channel-associated prepolymerized actin filaments, as actin polymerizes under the ionic strength conditions imposed in our study. This is supported in part by the lack of inhibition of G-actin in the presence of CD, which helps nucleate monomeric actin, and that of prepolymerized actin itself (Fig. 5). Regulation of cation channels in hST by gelsolin and Ca^{2+} further suggests an involvement of both actin and actin-binding proteins in the control of the actin networks present about, and interacting with, the cation channels in this syncytial epithelium. The hST apical membranes are expected to contain a number of functional channel species. However, several criteria strongly suggest that the cation channels studied in this report are the pool of cation channels, namely PC2, previously reported under control (spontaneously active) conditions (González-Perrett *et al.* 2001). The cytoskeleton-regulated channels were highly cation-selective (see reversal potential in a KCl gradient), and displayed a maximal conductance of 135 pS, and several substates, as reported (González-Perrett *et al.* 2001). The cytoskeleton-regulated cation channel activity was inhibited by La^{3+}, amiloride with an inhibitory constant identical to previously reported data, and anti-PC2 antibodies. Thus, the evidence as a whole is in agreement with a regulatory mechanism based on organized actin (F-actin) in the vicinity of PC2, the channel responsible for the electrodifussional K^+ and Ca^{2+} movement reported in the present study. This regulatory mechanism of hST cation channel activity is elicited by either disruption of endogenous actin filaments with CD, and/or addition of actin-binding proteins. Thus, it is likely that spontaneous channel activity, as previously reported, may have been elicited by changes in cytoskeletal structures brought about by vesicle formation. Recent findings (see accompanying manuscript submitted to *Hum. Mol. Genet.* Li *et al.* 2005) indicating that the actin-bundling protein α-actinin also regulates hST cation channel activity further support this contention. Interestingly, the effect of α-actinin was also tested and confirmed in isolated PC2, which was found to bind and is regulated by, this actin-associated protein. The presence of actin and actin-binding proteins in the hST membrane preparation is in agreement with an organized actin cytoskeleton in hST (Booth & Vanderpuye, 1983; Truman & Ford, 1984, 1986*a*,*b*; Demir *et al.* 1997; Kingdom *et al.* 2000) and hST vesicle preparations (Smith *et al.* 1977; Truman *et al.* 1981; Grosman *et al.* 1997). Interestingly, abundant α-actinin is found in apical, but not basolateral hST plasma membranes (Vanderpuye *et al.* 1986).

The human syncytiotrophoblast is a highly dynamic structure, whose function depends on the growth and branching of the invading trophoblast into the uterine mucosa (Ockleford *et al.* 1981; Kingdom *et al.* 2000). Changes in these highly coordinated morphological dynamics may be the effector of pathological features of the human placenta. The membrane–cytoskeleton functional interface may be critical for the cation-dependent signalling pathway(s) normally associated with various cell functions, including cell cycle, vesicle trafficking and ion transport. In this regard, Ca^{2+} plays a significant role in cellular function. A feedback mechanism linking Ca^{2+} transport to the cytoskeleton, and in particular

channel function, as described in this report, may be essential for other membrane-associated cell activities. A number of Ca^{2+}-binding proteins have been identified in the hST (Kenton *et al.* 1989; Kingdom *et al.* 2000), with strong interactions with the actin cytoskeleton and membrane-related events. These include the modulation of the phospholipase A2 inhibitor lipocortin II, and the Ca^{2+}-dependent phosphorylation of regulatory proteins (Kenton *et al.* 1989). Ca^{2+} signals have also been associated with channel regulation in placental preparations (Kibble *et al.* 1996), and the actin bundling protein α-actinin, for example, is released from the actin cytoskeleton in hST in a Ca^{2+}-dependent fashion (Vanderpuye *et al.* 1986). This is particularly interesting in the context of the present study, as α-actinin plays a role in the regulation of epithelial cation channels (Cantiello, 1995), and thus other Ca^{2+}-dependent feedback mechanisms may indeed be expected in term hST.

Recent studies from our laboratory determined that K^+ channel activity in hST is largely mediated by the gene product of the autosomal dominant polycystic kidney disease (ADPKD)-causing gene *PKD2*, the TRP-type channel PC2 (González-Perrett *et al.* 2001). Although little is known about the cytoskeletal interactions with PC2, recent studies suggest interactions between cytoskeletal components and PC2. Hax-1, a cytoskeletal protein that interacts with the F-actin-binding protein cortactin, interacts with PC2 (Gallagher *et al.* 2000). Moreover, we have recently found that two cytoskeletal-interacting proteins, troponin-I (Li *et al.* 2003*c*) and tropomyosin-1 (Li *et al.* 2003*a*) directly bind to PC2, further strengthening a link between cytoskeletal dynamics and PC2 in this epithelium. To date, the regulatory mechanisms that may entail cytoskeletal control of ion channel function in the onset and development of ADPKD are also largely unknown. Nonetheless, activation of the cAMP pathway, a manoeuvre that modifies the cytoskeleton (Hays *et al.* 1993; Prat *et al.* 1993), is an important regulatory signalling pathway in ADPKD cyst formation and expansion (reviewed in Sullivan *et al.* 1998). Interestingly, the actin cytoskeleton is implicated in the cAMP regulation of a number of channels (Prat *et al.* 1993, 1995, 1999), including ENaC and CFTR, which may be potential contributors to fluid accumulation in cyst formation. Recently, both proteins implicated in ADPKD, polycystin-1 (PC1) and PC2, were shown to colocalize with tubulin in cilia of renal epithelial cells (Yoder *et al.* 2002). Both proteins may play an important role in signalling events leading to volume flow stimulation of Ca^{2+} signals (Nauli *et al.* 2003). Thus, PC1/2 channel complexes may be part of a novel mechano-transduction signalling mechanism, which is regulated, or at least interacts with cytoskeletal structures.

In summary, our data demonstrate that channel-mediated K^+ and Ca^{2+} transport in hST, which is most likely to be mediated by a complex containing PC2, is controlled by cortical actin cytoskeleton, such that dynamic changes in actin-filament organization controls cation-channel gating and function. Disruption of endogenous actin filaments with CD, and/or addition of exogenous actin, both modify hST channel activity. This cytoskeletal control of cation channel activity in hST is further regulated by actin-binding proteins, including gelsolin, which severs prepolymerized actin filaments, and α-actinin, an abundant cytoskeletal component of the hST cytoskeleton (Vanderpuye *et al.* 1986). Whether other actin-associated proteins, including tropomyosin-1 (Li *et al.* 2003*a*) and troponin-I (Li *et al.* 2003*c*), which bind to the carboxy terminal end of PC2, may also have a regulatory role in channel function remains to be determined. Nevertheless, recent evidence indicates that the PC2-related polycystin-L is indeed controlled by troponin-I (Li *et al.* 2003*b*). Further studies will be required to determine whether any of these proteins is present and/or otherwise have a functional role in hST channel regulation. Both direct actin interactions, and cytoskeletal coupling through scaffolding proteins, may control channel activity in this syncytial epithelium. Conversely, other channel functions may also be targeted by the actin cytoskeleton. Cl^- channels, for example, are regulated by actin filaments (Schwiebert *et al.* 1994; Prat *et al.* 1995). It is thus possible, and rather likely, that the actin cytoskeleton may help concert various channel functions in the hST syncytial epithelium, as has been reported for other epithelial channels (Ismailov *et al.* 1997).

References

Beham A, Denk H & Desoye G (1988). The distribution of intermediate filament proteins, actin and desmoplakins in human placental tissue as revealed by polyclonal and monoclonal antibodies. *Placenta* **9**, 479–492.

Berdiev B, Prat AG, Cantiello HF, Ausiello DA, Fuller C, Jovov B, Benos DJ & Ismailov II (1996). Regulation of epithelial sodium channels by short actin filaments. *J Biol Chem* **271**, 17704–17710.

Bernucci L, Umana F, Llanos P & Riquelme G (2003). Large chloride channel from pre-eclamptic human placenta. *Placenta* **24**, 895–903.

Berryman M & Bretscher A (2000). Identification of a novel member of the chloride intracellular channel gene family (CLIC5) that associates with the actin cytoskeleton of placental microvilli. *Mol Biol Cell* **11**, 1509–1521.

Berryman M, Gary R & Bretscher A (1995). Ezrin oligomers are major cytoskeletal components of placental microvilli: a proposal for their involvement in cortical morphogenesis. *J Cell Biol* **131**, 1231–1242.

Bloxam DL, Bax BE & Bax CM (1997*a*). Culture of syncytiotrophoblast for the study of human placental transfer. Part II: Production, culture and use of syncytiotrophoblast. *Placenta* **18**, 99–108.

Bloxam DL, Bax CM & Bax BE (1997*b*). Culture of syncytiotrophoblast for the study of human placental transfer. Part I: Isolation and purification of cytotrophoblast. *Placenta* **18**, 93–98.

Booth GA, Olaniyan RO & Vanderpuye OA (1980). An improved method for the preparation of human placental syncytiotrophoblast microvilli. *Placenta* **1**, 327–336.

Booth AG & Vanderpuye OA (1983). Structure of human placental microvilli. *Ciba Found Symp* **95**, 180–194.

Bradford MM (1976). A rapid and sensitive method for the quantitation of microgram quantities of protein utilizing the principle of protein–dye binding. *Anal Biochem* **72**, 248–254.

Cantiello HF (1995). Role of the actin cytoskeleton on epithelial Na^+ channel regulation. *Kidney Int* **48**, 970–984.

Cantiello HF (1996). Role of the actin cytoskeleton in the regulation of the cystic fibrosis transmembrane conductance regulator. *Exp Physiol* **83**, 505–514.

Cantiello HF & Prat AG (1996). Role of actin filament organization in ion channel activity and cell volume regulation. In *Membrane Protein–Cytoskeleton Interactions*, vol. 43, ed. Nelson WJ, pp. 373–396. Academic Press, San Diego.

Cantiello HF, Stow J, Prat AG & Ausiello DA (1991). Actin filaments control epithelial Na^+ channel activity. *Am J Physiol Cell Physiol* **261**, C882–888.

Clark RK & Damjanov I (1985). Intermediate filaments of human trophoblast and choriocarcinoma cell lines. *Virchows Arch A Pathol Anat Histopathol* **407**, 203–208.

Demir R, Kosanke G, Kohnen G, Kertschanska S & Kaufmann P (1997). Classification of human placental stem villi: review of structural and functional aspects. *Microsc Res Tech* **38**, 29–41.

Douglas GC & King BF (1993). Colchicine inhibits human trophoblast differentiation in vitro. *Placenta* **14**, 187–201.

Enders AC (1965). Formation of syncitium from cytotrophoblast in the human placenta. *Obstet Gynecol* **25**, 378–386.

Gallagher AR, Cedzich A, Gretz N, Somlo S & Witzgall R (2000). The polycystic kidney disease protein PKD2 interacts with Hax-1, a protein associated with the actin cytoskeleton. *Proc Natl Acad Sci U S A* **97**, 4017–4022.

Goddette DW & Frieden C (1986). The kinetics of cytochalasin D binding to monomeric actin. *J Biol Chem* **261**, 15970–15973.

González-Perrett S, Batelli M, Kim K, Essafi M, Timpanaro GA, Montalbetti N, Reisin IL, Arnaout MA & Cantiello HF (2002). Voltage dependence and pH regulation of human polycystin-2 mediated cation channel activity. *J Biol Chem* **277**, 24959–24966.

González-Perrett S, Kim K, Ibarra C, Damiano AE, Zotta E, Batelli M, Harris PC, Reisin IL, Arnaout MA & Cantiello HF (2001). Polycystin-2, the protein mutated in autosomal dominant polycystic kidney disease (ADPKD), is a Ca^{2+}-permeable nonselective cation channel. *Proc Ntal Acad Sci U S A* **98**, 1182–1187.

Grosman C, Mariano MI, Bozzini JP & Reisin IL (1997). Properties of two multisubstate Cl^- channels from human syncytiotrophoblast reconstituted on planar lipid bilayers. *J Membr Biol* **157**, 83–95.

Grosman C & Reisin IL (2000). Single-channel characterization of a nonselective cation channel from human placental microvillus membranes. Large conductance, multiplicity of conductance states, and inhibition by lanthanides. *J Membr Biol* **174**, 59–70.

Hays R, Condeelis J, Gao Y, Simon H, Ding G & Franki N (1993). The effect of vasopressin on the cytoskeleton of the epithelial cell. *Pediatr Nephrol* **7**, 672–679.

Hesse M, Franz T, Tamai Y, Taketo MM & Magin TM (2000). Targeted deletion of keratins 18 and 19 leads to trophoblast fragility and early embryonic lethality. *EMBO J* **19**, 5060–5070.

Hille B (1992). *Ionic Channels of Excitable Membranes*, 2nd edn. Sinauer Associates, Sunderland, MA.

Ismailov II, Berdiev BK, Shlyonsky VG, Fuller CM, Prat AG, Jovov B, Cantiello HF, Ausiello DA & Benos DJ (1997). Role of actin in regulation of epithelial sodium channels by CFTR. *Am J Physiol Cell Physiol* **272**, C1077–1086.

Janmey P (1998). The cytoskeleton and cell signaling: component localization and mechanical coupling. *Physiol Rev* **78**, 763–781.

Johnson BD & Byerly L (1994). Ca^{2+} channel Ca^{2+}-dependent inactivation in a mammalian central neuron involves the cytoskeleton. *Pflugers Arch* **429**, 14–21.

Kaczan-Bourgois D, Salles JP, Hullin F, Fauvel J, Moisand A, Duga-Neulat I, Berrebi A, Campistron G & Chap H (1996). Increased content of annexin II (p36) and p11 in human placenta brush-border membrane vesicles during syncytiotrophoblast maturation and differentiation. *Placenta* **17**, 669–676.

Kenton P, Johnson PM & Webb PD (1989). The phosphorylation of p68, a calcium-binding protein associated with the human syncytiotrophoblast submembranous cytoskeleton, is modulated by growth factors, activators of protein kinase C and cyclic AMP. *Biochim Biophys Acta* **1014**, 271–281.

Kibble JD, Greenwood SL, Clarson LH & Sibley CP (1996). A Ca^{2+}-activated whole-cell Cl^- conductance in human placental cytotrophoblast cells activated via a G protein. *J Membr Biol* **151**, 131–138.

Kingdom J, Huppertz B, Seaward G & Kaufmann P (2000). Development of the placental villous tree and its consequences for fetal growth. *Eur J Obstet Gynecol Reprod Biol* **92**, 35–43.

Kwiatkowski D & Yin H (1987). Molecular biology of gelsolin, a calcium-regulated actin filament severing protein. *Biorheology* **24**, 643–647.

Lader AS, Kwiatkowski DJ & Cantiello HF (1999). Role of gelsolin in the actin filament regulation of cardiac L-type calcium channels. *Am J Physiol Cell Physiol* **277**, C1277–1283.

Li Q, Dai Y, Guo L, Liu Y, Hao C, Wu G, Basora N, Michalak M & Chen XZ (2003*a*). Polycystin-2 associates with tropomyosin-1, an actin microfilament component. *J Mol Biol* **325**, 949–962.

Li Q, Liu Y, Shen PY, Dai XQ, Wang S, Smillie LB, Sandford R & Chen XZ (2003*b*). Troponin I binds polycystin-L and inhibits its calcium-induced channel activation. *Biochemistry* **42**, 7618–7625.

Li Q, Shen PY, Wu G & Chen XZ (2003*c*). Polycystin-2 interacts with troponin I, an angiogenesis inhibitor. *Biochemistry* **42**, 450–457.

Li Q, Montalbetti N, Shen PY, Dai XQ, Cheeseman CI & Karpinski E *et al.* (2005). Alpha-actin in associates with polycystin-2 and regulates its channel activity. *Hum Mol Genet* **14**, 1587–1603.

Llanos P, Henriquez M & Riquelme G (2002). A low conductance, non-selective cation channel from human placenta. *Placenta* **23**, 184–191.

Maguire G, Connaughton V, Prat AG, Jackson GR Jr & Cantiello HF (1998). Actin cytoskeleton regulates ion channel activity in retinal neurons. *Neuroreport* **9**, 665–670.

Nauli SM, Alenghat FJ, Luo Y, Williams E, Vassilev P, Li X, Elia AEH, Lu W, Brown EM, Quinn SJ, Ingber DE & Zhou J (2003). Polycystins 1 and 2 mediate mechanosensation in the primary cilium of kidney cells. *Nat Genet* **33**, 129–137.

Ockleford CD, Wakely J & Badley RA (1981). Morphogenesis of human placental chorionic villi: cytoskeletal, syncytioskeletal and extracellular matrix proteins. *Proc R Soc Lond B Biol Sci* **212**, 305–316.

Ong AC, Ward CJ, Butler RJ, Biddolph S, Bowker C, Torra R, Pei Y & Harris PC (1999). Coordinate expression of the autosomal dominant polycystic kidney disease proteins, polycystin-2 and polycystin-1, in normal and cystic tissue. *Am J Pathol* **154**, 1721–1729.

Parast MM & Otey CA (2000). Characterization of palladin, a novel protein localized to stress fibers and cell adhesions. *J Cell Biol* **150**, 643–656.

Prat AG, Bertorello AM, Ausiello DA & Cantiello HF (1993). Activation of epithelial Na^+ channels by protein kinase A requires actin filaments. *Am J Physiol Cell Physiol* **265**, C224–233.

Prat AG, Cunningham CC, Jackson Jr GR, Borkan S, Wang Y, Ausiello DA & Cantiello HF (1999). Actin filament organization is required for proper cAMP-dependent activation of CFTR. *Am J Physiol Cell Physiol* **277**, C1160–1169.

Prat AG, Xiao YF, Ausiello DA & Cantiello HF (1995). cAMP-independent regulation of CFTR by the actin cytoskeleton. *Am J Physiol Cell Physiol* **268**, C1552–1561.

Reczek D, Berryman M & Bretscher A (1997). Identification of EBP50: a PDZ-containing phosphoprotein that associates with members of the ezrin-radixin-moesin family. *J Cell Biol* **139**, 169–179.

Schwiebert EM, Mills JW & Stanton BA (1994). Actin-based cytoskeleton regulates a chloride channel and cell volume in a renal cortical collecting duct cell line. *J Biol Chem* **269**, 7081–7089.

Smith CH, Nelson DM, King BF, Donohue TM, Ruzycki S & Kelley LK (1977). Characterization of a microvillous membrane preparation from human placental syncytiotrophoblast: a morphologic, biochemical, and physiologic, study. *Am J Obstet Gynecol* **128**, 190–196.

Snedecor GW & Cochran WG (1973). *Statistical Methods*. Iowa State University Press, Ames, Iowa.

de Souza PC & Katz SG (2001). Co-expression of cytokeratin and vimentin in mice trophoblastic giant cells. *Tissue Cell* **33**, 40–45.

Stulc J (1997). Placental transfer of inorganic ions and water. *Physiol Rev* **77**, 805–836.

Sullivan LP, Wallace DP & Grantham JJ (1998). Epithelial transport in polycystic kidney disease. *Physiol Rev* **78**, 1165–1191.

Truman P & Ford HC (1984). The brush border of the human term placenta. *Biochim Biophys Acta* **779**, 139–160.

Truman P & Ford HC (1986*a*). Proteins of human placental microvilli. I. Cytoskeletal proteins. *Placenta* **7**, 95–110.

Truman P & Ford HC (1986*b*). Proteins of human placental microvilli. II. Identification and topology of the plasma membrane proteins. *Placenta* **7**, 111–120.

Truman P, Wakefield JS & Ford HC (1981). Microvilli of the human term placenta. Isolation and subfractionation by centrifugation in sucrose density gradients. *Biochem J* **196**, 121–132.

Undrovinas A, Shander G & Makielski J (1996). Cytoskeleton modulates gating of voltage-dependent Na^+ channels in heart. *Am J Physiol Heart Circ Physiol* **269**, H203–214.

Vanderpuye OA, Edwards HC & Booth AG (1986). Proteins of the human placental microvillar cytoskeleton. alpha-actinin. *Biochem J* **233**, 351–356.

Xu GM, González-Perrett S, Essafi M, Timpanaro GA, Montalbetti N, Arnaout MA & Cantiello HF (2003). Polycystin-1 activates and stabilizes the polycystin-2 channel. *J Biol Chem* **278**, 1457–1462.

Yin HL, Albretch JH & Fattoum A (1981). Identification of gelsolin, a Ca^{2+}-dependent regulatory protein of actin gel-sol transformation, and its intracellular distribution in a variery of cells and tissues. *J Cell Bol* **91**, 901–908.

Yoder BK, Hou X & Guay-Woodford LM (2002). The polycystic kidney disease proteins, polycystin-1, polycystin-2, polaris, and cystin, are co-localized in renal cilia. *J Am Soc Nephrol* **13**, 2508–2516.

Acknowledgements

H.F.C. was funded by the Polycystic Kidney Disease Foundation. X.-Z. Chen and his group were supported by the Canadian Institutes for Health Research, the Alberta Heritage Foundation for Medical Research, and the Heart and Stroke Foundation of Canada. Q.L. is a recipient of the Kidney Foundation of Canada Biomedical Fellowship. A preliminary report of this study was presented at the 1st Latino American Symposium of the International Society of Placenta, Sao Paulo, 2003. The authors thank Jimena Semprine, María del Rocío Cantero and Gustavo A. Timpanaro for most willing and helpful technical support.